Use of Fourier transform infrared microscopy for the evaluation of drug efficiency

Vitaly Erukhimovitch
Marina Talyshinsky
Yelena Souprun
Mahmoud Huleihel
Ben Gurion University of the Negev
The National Institute for Biotechnology
Department of Virology and Developmental Genetics
Beer-Sheva, Israel

Abstract. Fourier transform infrared (FTIR) spectroscopy has been used by chemists as a powerful tool to characterize inorganic and organic compounds. In this study, we examine the potential of FTIR microspectroscopy for early evaluation of therapy efficiency. For this purpose, we examine the effect of acyclovir (a known antiherpetic drug) on the development of herpes simplex virus type 1 (HSV-1) infection in cell culture. Also, we examine spectral changes in lymphocytes obtained from leukemia patients after appropriate chemotherapy treatment. Our results show early and significant spectral indicators for successful infection of Vero cells with HSV-1. Treatment of these infected cells with increasing doses of acyclovir reduces clearly the spectral changes caused by the infection in a correlation with inhibiting the development of the cytopathic effect (CPE) induced by this virus. Also significant and consistent spectral differences between lymphocytes from human leukemia patients compared to that from healthy persons are obtained. Treatment of these leukemia patients with appropriate drugs reduces significantly these spectral differences in a correlation with the improvement of the patient's clinical situation. It seems that FTIR spectroscopy can be used as an effective tool for early evaluation of the efficiency of drugs. *© 2006 Society of Photo-Optical Instrumentation Engineers.* [DOI: 10.1117/1.2397554]

Keywords: Fourier transform infrared microspectroscopy; herpes simplex virus type 1; drug efficiency; acyclovir; leukemia.

Paper 06081R received Apr. 2, 2006; revised manuscript received Jul. 25, 2006; accepted for publication Jul. 25, 2006; published online Nov. 22, 2006.

1 Introduction

In general, early diagnosis and appropriate treatment increase dramatically the chances of survival and full recovery from various serious diseases.[1–4] For instance, despite the improvement in diagnostic techniques, the vast majority of cancers have either advanced or metastasized by the time they are diagnosed.[5] Hence, there is a need to develop novel noninvasive diagnostic methods to detect the malignancy and probably other serious diseases in the earlier stages and start an appropriate and effective treatment. Death rates and costs associated with infectious diseases could be significantly reduced by employing rapid identification techniques and precise methods for evaluation of the efficiency of the therapy used.[3,6]

Fourier transform infrared (FTIR) spectroscopy has been widely applied in biology and medicine. It has expanded our knowledge of the structure, conformation, and dynamics of various molecular components of the cell.[7] With the introduction of microscopy in modern FTIR instrumentation, FTIR analysis of cells and tissues has become a reality. In recent years, there is bubbling interest to apply FTIR spectroscopy as a tool for the diagnosis of cancer. Successful diagnostic studies of different kinds of cancer cells and cells infected with viruses have been reported.[8–12] Besides the application of FTIR spectroscopy to cell and tissue diagnostics, its role in diagnostic aspects involving body fluids has been gaining importance in the last few years. Successful diagnosis of arthritis based on near-IR (NIR) analysis of synovial fluid obtained from patients has been reported.[13] The mid-IR region has been shown to be useful in the identification of disease patterns using the FTIR spectrum of human sera.[14] Precise quantification of serum components such as glucose, total protein, cholesterol, and urea have been achieved using mid-IR spectroscopy.[15,16] Also FTIR spectroscopy was used successfully for identification and finger printing of micro-organisms.[3,17,18]

In the present study, we examined the potential of FTIR microscopy methods for the evaluation of drug efficiency.

2 Materials and Methods

2.1 *Cells, Viruses, and Treatment*

African green monkey kidney (Vero) cells were purchased from the American Type Culture Collection (ATCC), Rockville, Maryland. Cells were grown in Dulbecco's modified Eagle's medium (DMEM) containing 10% fetal calf serum (FCS), 1% glutamine, 50-U/ml penicillin, and 50-μg/ml

Address all correspondence to Mahmoud Huleihel, Virology @ Developmental Genetics and Institute of Applied Biosciences, Ben-Gurion Univ. of the Negev, Sderot Ben Gurion, Beer Sheva, Negev 84105 Israel; Tel: +97286461999; Fax: +97286472970; E-mail: mahmoudh@bgu.ac.il

1083-3668/2006/11(6)/064009/6/$22.00 © 2006 SPIE

streptomycin, and incubated at 37°C in humidified air containing 5% CO_2. Vero cells were used for the infection of herpes simplex virus type 1 (HSV-1). HSV-1 was obtained from ATCC (VR-735).

HSV-1 infected cells were treated with various concentrations (0.1, 1, and 10 μM) of the known antiherpetic drug acyclovir (ACV) immediately postinfection (PI). The treatment continued up to the end of the experiment.

Human lymphocytes were isolated from ten healthy persons and ten leukemia patients. Both healthy persons and leukemia patients were 10 to 30 years old. Standard chemotherapy treatment was given to the leukemia patients.[19]

2.2 *Cell Infection and Determination of Cytopathic Effect*

Monolayers of Vero cells (seeded at 1.5×10^5 cells/well on 24-well culture plates) were incubated with HSV-1 at the appropriate multiplicity of infection (1 MOI) in RPMI medium containing 2% FCS at 37°C for 2 h. The unabsorbed virus particles were removed, fresh medium containing 2% FCS with or without various concentrations of the antiherpetic drug acyclovir (ACV) was added, and the cell monolayers were incubated at 37°C. At the required time, the CPE in cell culture was examined under an inverted microscope.

2.3 *Isolation of Lymphocytes*

Lymphocytes were isolated as previously described.[20] Briefly, 3 ml of blood was loaded over 3 ml of Histopaque (purchased from Sigma, St. Louis, Missouri) solution and centrifuged at 300 g for 30 min at 23°C. The Histopaque solution is the mixture of Metrizoic acid and Ficoll solution having density of 1.077 g/ml. The lymphocyte layer (mononuclear cells), located at the middle of the tube, was isolated. The separated lymphocytes were washed twice with 10 ml of saline by centrifugation at 300 g for 10 min at 23°C, and resuspended in 100 μL of saline solution. The cells were counted with a hematocytometer, and all tested samples were centrifuged again and resuspended in saline solution at a concentration of 1000 cells/ml.

2.4 *Preparation of Infected and Uninfected Vero Cells for Examination by Fourier Transform Infrared Microscopy*

Infected and uninfected Vero cell monolayers were washed twice with saline and the cells were picked up from the tissue culture plates after treatment with trypsin (0.25%) for 1 min. The cells were pelleted by centrifugation at 1000 rpm for 5 min. Each pellet was washed twice with saline and resuspended in 100 μl of saline. The number of cells was counted with a hematocytometer, and all tested samples were pelleted again and resuspended in an appropriate volume of saline to give a concentration of 1000 cells/μl.

2.5 *Preparation of Slides for Examination by Fourier Transform Infrared Microscopy*

Since ordinary glass slides exhibit strong absorption in the wavelength range of interest to us, we used zinc selenide crystals, which are highly transparent to IR radiation. A drop of 1 μl of each sample (lymphocytes or Vero cell suspensions) was placed on the zinc selenide crystal, air dried for 4 h, and examined by FTIR microscopy. The radius of such a 1-μl drop was about 1 mm.

2.6 *Fourier Transform Infrared Spectra*

FTIR measurements were performed in transmission mode with a liquid nitrogen-cooled mercury cadmium telluride (MCT) detector of FTIR microscope (Bruker IRScope II) coupled to the FTIR spectrometer (Bruker Equinox model 55/S, Opus software) (Ettlingen, Germany). The spectra were obtained in the wavenumber range of 600 to 2000 cm^{-1} in the mid-IR region. A spectrum was taken as an average of 128 scans to increase the signal-to-noise ratio (SNR), and the spectral resolution was 4 cm^{-1}. The aperture used in this study was 100 μm, since we found that this aperture gives the best SNR. At lower apertures, the quality of spectra was bad due to high levels of noise. The cells in the chosen apertures are homogeneous without impurities (such as salts, media components, etc.) and the number of cells in such apertures is about 100. Baseline correction and normalization were performed for all the spectra by Opus software. Baseline correction was done by rubberband method. For the construction of the baseline, the spectrum is divided up in n ranges of equal size. In each range, the minimum y value is determined. The baseline is created by connecting minima with straight lines. Starting from "below," a rubberband is stretched over this curve. The rubber band is the baseline. The baseline points that do not lie on the rubberband are discarded. Normalization was done by vector method. The average y value of the spectrum is calculated first. This average value is then subtracted from the spectrum so that the middle of the spectrum is pulled down to $y=0$. The sum of the squares of all y values is then calculated, and the spectrum is divided by the square root of this sum. The vector norm of the result spectrum is 1. Peak positions were determined using the second derivation method by Opus software. For each cell type, the spectrum was taken as the average of five different measurements at various sites of the sample.

Each experiment with each cell type was repeated five times and 25 measurements were obtained from each sample. It is important to mention that there are no considerable differences in spectra from various sites of the same sample; standard deviation (SD) did not exceed 0.005.

2.7 *Cluster Analysis*

Among the various mathematical methods applied for classification in biology and medicine, cluster analysis is one of the simplest and most rapid procedures.[21] In our study, this technique was used to classify certain regions of the FTIR spectra of the examined samples. Cluster analysis was performed by Opus software with a standard making-distance matrix and Ward's algorithm dendrogram.

3 Results

3.1 *Fourier Transform Infrared Spectra of Infected Cells with Herpes Simplex Virus Type 1*

Vero cells were infected with HSV-1 and examined by FTIR microscopy at 24 and 48 h postinfection (PI), and their spectral behavior was examined by FTIR microscopy. The results

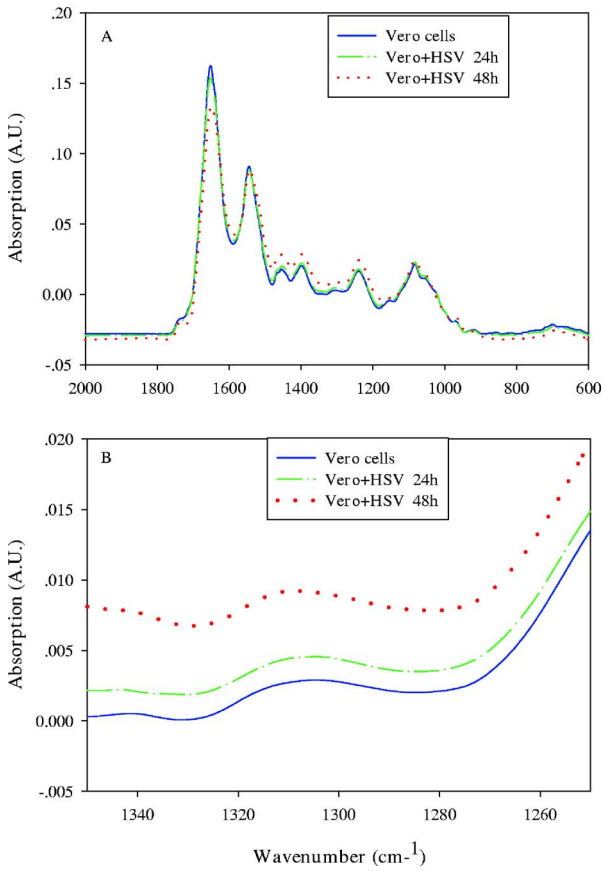

Fig. 1 (a) FTIR spectra in the region 600 to 2000 cm^{-1} of control Vero cells, with cells infected with HSV-1 at 24- and 48-h PI. (b) FTIR microspectroscopy in the region 1250 to 1350 cm^{-1} for the tested cells. Data are means of five different and separate experiments for each cell culture.

presented in Fig. 1(a) showed the FTIR spectra of both control and infected Vero cells at 24 and 48 h PI. In general, the infected cells show higher intensities of absorbance at various regions of the scanned area. For both normal and HSV infected cells, the dominant bands at 1655 and 1546 cm^{-1} were attributed to protein amide 1 and 2 bands.[1] The shoulder at about 1730 cm^{-1} was attributed to lipid C═O stretching vibrations.[1] The band at 1465 cm^{-1} was assigned to the CH_2 bending mode of the cell lipids. The bands at 1454 and 1397 cm^{-1} were attributed to asymmetric and symmetric CH_3 bending modes of end ethyl groups and branched methyl groups of proteins and lipids, respectively.[22] The peaks at 1237 and 1082 cm^{-1} were attributed to asymmetric and symmetric stretching vibrations and phospholipids.[1,23] The peak at 1064 cm^{-1} resulted from the overlap of several bands, including absorption due to the vibrational modes of $-CH_2OH$ and the C-O stretching vibration coupled to the C-O bending mode of cell carbohydrates.[24] The peak at 857 cm^{-1} was attributed to N-type sugars.[25]

A considerable gradual absorption increase in the region 1250 to 1350 cm^1 at the various examined times PI was observed in all infected cell cultures [Fig. 1(b)]. Furthermore, the position of the peak at 857 cm^{-1} in noninfected control cells was gradually shifted to about 854 cm^{-1} in infected cells, in correlation with the development of the viral infection (Table 1). These parameters were used for follow up after the development of the viral infection in the next experiments of this study.

Table 1 Changes in peak position at 857 cm^{-1} in HSV-1 infected Vero cells treated or untreated with various concentrations of ACV.

	Peak position (cm^{-1})	
Cells	24 h PI	48 h PI
Control Vero	857.7 ± 0.2	857.8 ± 0.2
Vero+ HSV	855.4 ± 0.25	854.2± 0.2
Vero+ HSV+ 0.1 μM ACV	856.4 ± 0.3	855.3± 0.25
Vero+ HSV+ 1 μM ACV	857.1± 0.27	855.8± 0.2
Vero+HSV+ 10 μM ACV	857.3± 0.26	856.2± 0.3

Vero cells were infected with 1 MOI of HSV-1 and treated immediately PI with different concentrations of ACV and examined by FTIR microscopy at 24- and 48-h PI. The results are means ±*SD*, (*n*=5).

3.2 *Treatment of Herpes Simplex Virus Type 1 Infected Vero Cells with Antiherpetic Drug Acyclovir*

Vero cells were infected with HSV-1 and treated immediately PI with increasing concentrations of ACV. The FTIR spectra obtained at 48-h PI of these cells show spectral intensity values at regions 1250 to 1350 cm^1 lower than those of the infected nontreated cells but slightly higher than the control uninfected cells, according to the used concentrations of ACV (Fig. 2). At concentrations of 1 and 10 μM of ACV, the spectral results of the infected and treated cells demonstrated only a slight increase compared to the control uninfected cells, while at the lower used concentration of 0.1 μM, there is a further increase in the spectral intensity values at this region (Fig. 2). The results presented in Table 1 show only a moderate shift of peak at 857-cm^{-1} position in infected and treated cells compared to the infected nontreated cells. This shift is also dependent on the concentration of the used ACV, while it is smaller in the higher drug concentrations.

In addition, the results presented in Fig. 2 show the possibility of follow up after the effect of the used drug as a function of time PI. It can be seen from these results that at 24-h PI, the spectra of the infected and treated cells with 1 and 10 μM of ACV in regions 1250 to 1350 cm^{-1} are fully similar to the control uninfected cells, while the infected untreated cells show significantly higher values of the spectra. At this point of time, it can be seen that in infected cells treated with 0.1 μM of ACV, the spectral values already start to increase. At 48 h, there is only a slight increase in the spectral levels of cells infected and treated with either 1 or 10 μM of ACV, compared to the control uninfected cells, while in those treated with 0.1 μM, there is a notable increase in the spectra levels. Full and excellent classification of all infected and treated samples with 1 μM of ACV compared to the control infected and untreated samples was obtained in the region 1280 to 1350 cm^{-1} by cluster analysis (Fig. 3).

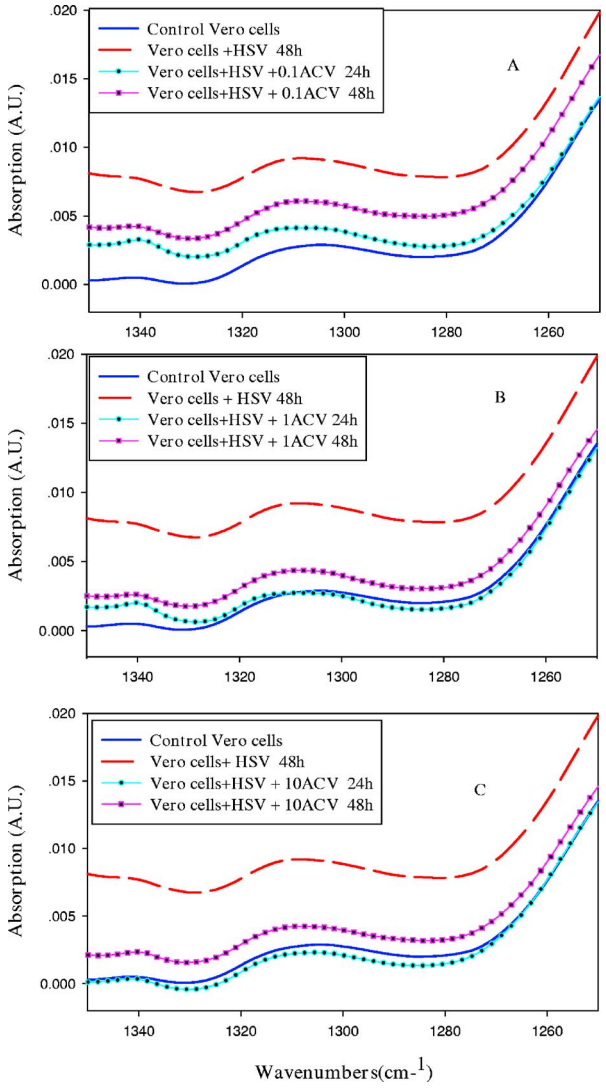

Fig. 2 (a) FTIR spectra in the region 1250 to 1350 cm^{-1} of control Vero cells, with cells infected with HSV-1 at 48-h PI, cells infected with HSV-1 and treated with 0.1-μM ACV at 24-h PI, and cells infected with HSV-1 and treated with 0.1-μM ACV at 48-h PI. (b) Same as (a) but treated with 1-μM ACV. (c) Same as (a) but treated with 10-μM ACV. Data are means of five different and separate experiments for each cell culture.

These results are in agreement with the observed morphological changes [cytopathic effect (CPE) development] of the infected cells (Fig. 4), although spectral changes are detectable significantly earlier than morphological changes. The results in Fig. 4 show that the CPE is observed in the infected nontreated cells only 48-h PI, while the spectroscopic changes are measured earlier at 24 h, as shown in Fig. 1. Also, in the case of infected and treated cells with the various concentrations of ACV, low levels of CPE were observed only at 72 to 90-h PI in cells treated with 1 or 10 μM of ACV and at 48 to 60 h in those treated with 0.1 μM.

3.3 *Spectral Behavior of Leukemia Lymphocytes Before and After Chemotherapy Treatment*

Lymphocytes were isolated from healthy persons and from leukemia patients before and after a course of chemotherapy

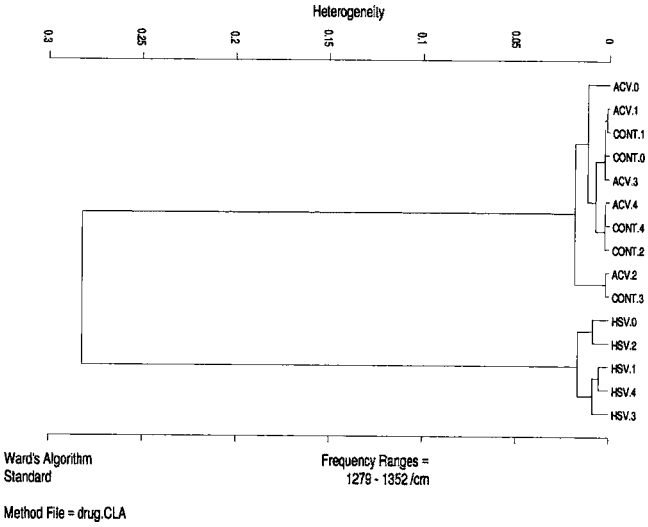

Fig. 3 Cluster analysis of the IR spectra of the examined control uninfected and HSV-1 infected treated or untreated cells with 1-μM ACV in the frequency range 1280 to 1350 cm^{-1}. This cluster analysis was made on results obtained at 48-h PI. Five samples from each kind of cell, control uninfected (CONT), infected (HSV-1), and infected and treated with ACV (ACV) were examined.

treatment, and their spectral behavior was examined by FTIR microscopy. Our results show significant and remarkable differences between normal and leukemia lymphocytes (Fig. 5). Some of these differences are represented by a significant reduction in the intensity of the absorbance due to a PO_2-asymmetric stretching band (in the region 1250 to 1350 cm^{-1}) for leukemia lymphocytes compared to normal lymphocytes [Fig. 5(b)].

Also, our measurements show a considerable and detectable shift of the peak at 1082 to 1083 cm^{-1} (which represent the PO_2-symmetric stretching band) for the normal lymphocytes 1086 to 1087 cm^{-1} in leukemia lymphocytes [Fig. 5(c)].

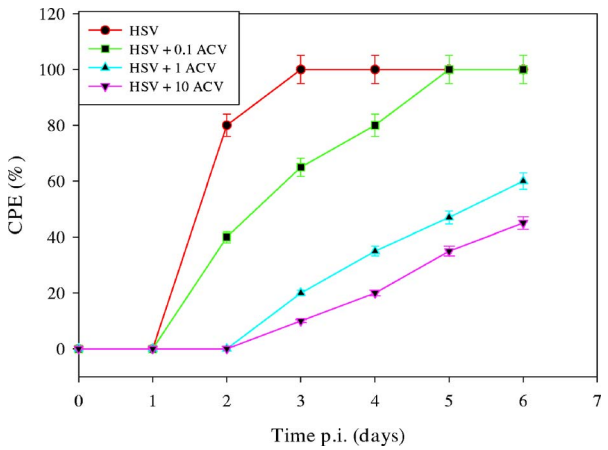

Fig. 4 Effect of ACV on the kinetics of CPE development after infection with HSV-1. Vero cells were infected with 1 MOI of HSV-1 and treated with various concentrations of ACV immediately PI. CPE was evaluated by inverted microscope observations. Data are means ±*SD* (*n*=5).

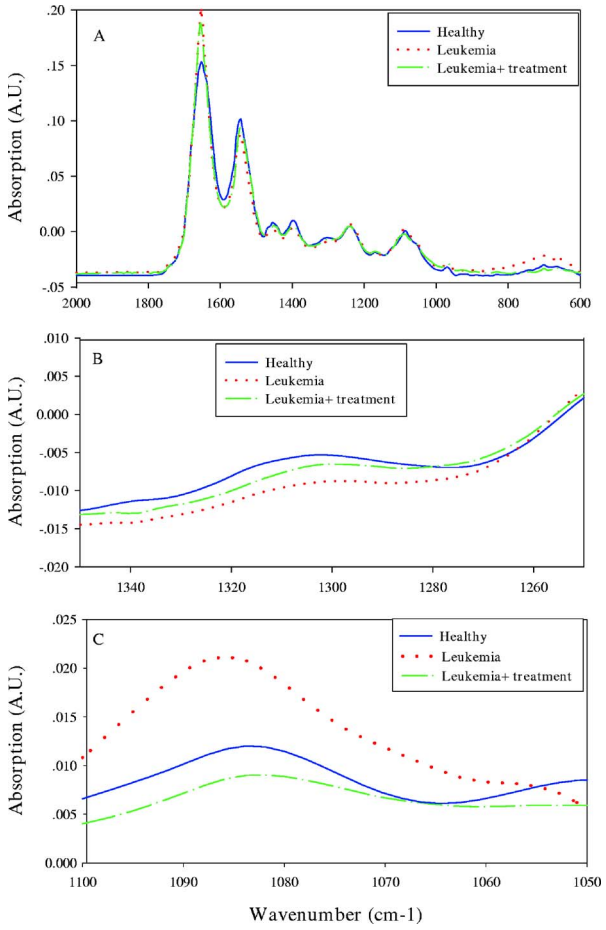

Fig. 5 (a) FTIR spectra in the region 600 to 2000 cm^{-1} of lymphocytes obtained from healthy persons, leukemia patients, and leukemia patients after 1 week of treatment with the appropriate drug. (b) FTIR spectra in the region 1250 to 1350 cm^{-1} of the same cells in (a). (c) FTIR spectra in the region 1050 to 1100 cm^{-1} of the same cells in (a). Data are means of ten different samples from either healthy persons or leukemia patients.

Our results show that lymphocytes from leukemia patients became very similar to normal lymphocytes in their IR spectra at the end of treatment, as can be seen in Fig. 5. The results presented in Figs. 5(b) and 5(c) show that both the position of the PO_2-symmetric stretching band and the intensity of PO_2 - asymmetric stretching in the treated leukemia lymphocytes goes in the direction of their values in normal lymphocytes.

4 Discussion

For the past few years, the application of FTIR spectroscopy in the biomedical field, particularly in the detection and identification of cancer cells and micro-organisms, has become increasingly interesting.[1,3] The introduction of microscopy to the traditional FTIR instrument makes it possible to focus on a specific small region of the slide and to use only very small aliquots of samples.

The main objective of the present study is to examine the potential of FTIR microscopy as a rapid and reliable method for evaluation of the efficacy of the used therapy. For this purpose, we used Vero cells that were infected *in vitro* with HSV-1 (with or without treatment with the known antiherpetic drug ACV) and lymphocytes isolated from leukemia patients before and after appropriate chemotherapy treatment.

The results presented in this study proved the potential of FTIR microscopy for rapid and reliable detection of both infected cells with HSV-1 and leukemia lymphocytes, and for early evaluation of the efficiency of the used therapy. This study is considered one of the first studies introducing an easy and rapid technique for the evaluation of the efficacy of the used therapy, which can be critical for life saving.

It is seen that different spectral peaks over the FTIR spectra of the examined samples can be used as excellent biomarkers for the identification of these samples and as indication for the efficiency of the used drugs. For instance, the spectral absorbance values in the phosphate region (1250 to 1350 cm^{-1}) significantly increase in cells infected with HSV-1, while they significantly decrease in leukemia lymphocytes [Figs. 1(b) and 4(b)]. The peak at the 857-cm^{-1} position in control Vero cells was shifted to the 854-cm^{-1} position in HSV-1 infected cells. These changes were significantly reduced according to the used concentration of the drug, while they are smaller in the higher drug concentrations (Table 1 and Figs. 2 and 5). These results are in agreement with our work and other previous studies.[1,12]

Another important biomarker for the detection of leukemia lymphocytes is a significant and detectable shift of the peak at 1082 to 1083 cm^{-1} (which represent the PO_2-symmetric stretching band) for the normal lymphocytes to 1086 to 1087 cm^{-1} in leukemia lymphocytes, as can be seen from Fig. 2 and from other previous studies.[24] The shift in this peak may indicate that the environment near the PO_2- group has undergone a series of alterations during malignancy, or that there were changes in the concentrations of some metabolites such as carbohydrates, which could be related to tumor development and/or to the high rate of replication of these cells, i.e., the high rate of DNA synthesis in the malignant cells.[26] This shift disappeared completely in lymphocytes obtained from leukemia patients at the end of their chemotherapy treatment course [Fig. 5(c)].

These biomarkers could be used successfully for follow up after efficacy of the used drug, and might be useful for evaluation and determination of the required doses of the used drug. In HSV infected cells and those treated with ACV, there is a good correlation between drug dose and the reduction in the intensity of the spectral changes caused by the HSV-1 infection. It can be seen from Fig. 2 and Table 1 that the obtained spectra of HSV infected cells that were treated with either of the higher doses 1 or 10 μg/ml of ACV were very similar to that of the uninfected control cells, whereas the lower dose (0.1 μg/ml) of ACV shows significant difference compared to the uninfected control cells, as can be seen in Fig. 2. These results mean that ACV at high doses (1 and 10 μg/ml) is highly effective in blocking the viral infection, while at the low dose (0.1 μg/ml) it is not fully effective. These results, which are in agreement with the morphological changes, might indicate the possible use of FTIR spectroscopy for early and rapid determination of the effective required doses of drugs. In addition, the spectral changes of the infected cells were detectable as early as 24-h PI, while the

observed morphological changes were obtained only at 2 to 3 days PI (Figs. 2 and 4).

The present study strongly supports the possibility of developing FTIR microscopy for the detection and identification of diseases, and as an indication of efficiency of treatment.

References

1. R. K. Dukor, in *Handbook of Vibrational Spectroscopy*, J. M. Chalmers and P. R. Griffiths, Eds., pp. 3335–3360, John Wiley and Sons, New York (2001).
2. L. A. G. Ries, C. L. Kosary, B. F. Hankey, B. A. Miller, L. Clegg, and B. K. Edwards, *Seer Cancer Statistics Review*, pp. 197–205, National Cancer Institute, Bethesda, MD (1999).
3. K. Maquelin, C. Kirschner, L. P. Choo-Smith et al., "Prospective study of the performance of vibrational spectroscopies for rapid identification of bacterial and fungal pathogens recovered from blood cultures," *J. Clin. Microbiol.* **41**, 324–429 (2003).
4. J. M. Miller and C. M. O'Hara, in *Manual of Clinical Microbiology*, P. R. Murray, E. J. Baron, M. A. Pfaller, F. C. Tenover, and R. H. Yolken, Eds., pp. 193–201, ASM Press, Washington, DC (1999).
5. T. Burmeister, "Oncogenic retroviruses in animals and humans," *Rev. Med. Virol.* **11**, 369–380 (2001).
6. M. Essendoubi, D. Toubas, M. Bouzaggou, J. M. Pinon, and M. Manfait, "Rapid identification of candida species by FTIR microscopy," *Biochim. Biophys. Acta* **1724**, 239–247 (2005).
7. H. Mantsch and D. Chapman, *Infrared Spectroscopy of Biomolecules*, Chap. 2, pp. 6–9, John Wiley, New York (1996).
8. H. P. Wang, H. C. Wang, and Y. J. Huang, "Microscopic FTIR studies of lung cancer cells in pleural fluid," *Sci. Total Environ.* **204**, 283–287 (1997).
9. T. Gao, J. Feng, and Y. Ci, "Human breast carcinomal tissues display distinctive FTIR spectra: implication for the histological characterization of carcinomas," *Anal Cell Pathol.* **18**, 87–93 (1999).
10. B. Rigas, K. LaGuardia, L. Qiao, B. S. Bhandare, T. Caputo, and M. A. Cohenford, "Infrared spectroscopic study of cervical smears in patients with HIV: implications for cervical carcinogenesis," *J. Lab. Clin. Med.* **35**, 26–31 (2000).
11. V. Erukhimovitch, M. Talyshinsky, Y. Souprun, and M. Huleihel, "Spectroscopic characterization of human and mouse primary cells, cell lines and malignant cells," *Photochem. Photobiol.* **76**, 446–451 (2002).
12. M. Huleihel, M. Talyshinsky, Y. Souprun, and V. Erukhimovitch, "Spectroscopic evaluation of cells infected with herpes viruses and treated with red microalgal polysaccharides," *Appl. Spectrosc.* **57**, 390–395 (2003).
13. R. A. Shaw, S. Kotowich, H. H. Eysel, M. Jackson, G. H. Thomson, and H. H. Mantsch, "Arthritis diagnosis based upon the near-infrared spectrum of synovial fluid," *Rheumatol. Int.* **15**, 159–165 (1995).
14. A. Staib, B. Dolenko, D. L. Fink, J. Fruh, A. E. Nikulin, M. Otto, M. S. Pessin-Minsley, O. Quarder, R. Somorjai, U. Thienel, and G. Werner, "Disease pattern recognition testing for rheumatoid arthritis using infrared spectra of human serum," *Clin. Chim. Acta* **308**, 79–89 (2001).
15. R. A. Shaw, S. Kotowich, M. Leroux, and H. H. Mantsch, "Multianalyte serum analysis using mid-infrared spectroscopy," *Ann. Clin. Biochem.* **35**, 624–632 (1998).
16. C. Petibois, G. Cazorla, H. Gin, and G. Deleris, "Differentiation of populations with different physiologic profiles by plasma Fourier-transform infrared spectra classification," *J. Lab. Clin. Med.* **137**, 184–190 (2001).
17. V. Erukhimovitch, V. Pavlov, M. Talyshinsky, Y. Souprun, and M. Huleihel, "FTIR microscopy as a method for identification of bacterial and fungal infections," *J. Pharm. Biomed. Anal* **37**, 1105–1108 (2005).
18. D. Naumann, D. Helm, and H. Labischinski, "Microbiological characterizations by FT-IR spectroscopy," *Nature (London)* **351**, 81–82 (1991).
19. R. Sahu, U. Zelig, M. Huleihel, N. Brosh, M. Talyshinsky, M. Ben-Harosh, S. Mordechai, and J. Kapelushnik, "Continuous monitoring of WBC (biochemistry) in an adult leukemia patient using advanced FTIR-microspectroscopy," *Leuk. Res.* **30**, 687–693 (2006).
20. J. Ramesh, M. Huleihel, J. Mordechai, A. Moser, V. Erukhimovitch, C. Levi, J. Kapelushnik, and S. Mordechai, "Preliminary results of evaluation of progress in chemotherapy treatment for childhood leukemia patients employing FTIR microspectroscopy and cluster analysis," *J. Lab. Clin. Med.* **141**, 385–394 (2003).
21. C. Kristensen, N. Ashkenasy, R. Jain, and A. Koretsky, "Creatine and cyclocreatine treatment of human colon adenocarcinoma xenografts: ^{31}P and ^{1}H magnetic resonance spectroscopic studies," *Br. J. Cancer* **79**, 278–285 (1999).
22. P. Wong, S. Goldstein, R. Grekin, A. Godwin, C. Pivik, and B. Rigas, "Distinct infrared spectroscopic patterns of human basal cell carcinoma of the skin," *Cancer Res.* **53**, 762–765 (1993).
23. R. R. Dukor, M. N. Liebman, and B. L. Johnson, "A new nondestructive method for analysis of clinical samples with FT-IR microspectroscopy. Breast cancer tissue as an example," *Cell Mol. Biol. (Paris)* **44**, 211–217 (1998).
24. D. Yang, D. Castro, I. El-Sayed, M. El-Sayed, R. Saxton, and N. Y. Zhang, "A Fourier-transform infrared spectroscopic comparison of cultured human fibroblast and fibrosarcoma cells: a new method for detection of malignancies," *J. Clin. Laser Med. Surg.* **13**, 55–59 (1995).
25. A. E. Taillandier and J. Liguier, in *Handbook of Vibrational Spectroscopy*, J. M. Chalmers and P. R. Griffiths, Eds., pp. 3465–3480, John Wiley and Sons, New York (2001).
26. H. Susi, in *Structure and Stability of Biological Macromolecules*, S. N. Timashett and C. D. Fasman, Eds., pp. 641–652, Marcel Dekker, New York (1969).